

A Stable Water Chain in the Hydrophobic Pore of the AmtB Ammonium Transporter

Guillaume Lamoureux,* Michael L. Klein,* and Simon Bernèche[†]

*Center for Molecular Modeling, Department of Chemistry, University of Pennsylvania, Philadelphia, Pennsylvania; and

[†]Biozentrum, University of Basel, Basel, Switzerland

ABSTRACT The accessibility of water molecules to the pore of the AmtB ammonium transporter is studied using molecular dynamics simulations. Free energy calculations show that the so-called hydrophobic pore can stabilize a chain of water molecules in a well of a few kcal/mol, using a favorable electrostatic binding pocket as an anchoring point. Moreover, the structure of the water chain matches precisely the electronic density maxima observed in x-ray diffraction experiments. This result questions the general assumption that the AmtB pore only contains ammonia (NH₃) molecules diffusing in a single file fashion. The probable presence of water molecules in the pore would influence the relative stability of NH₃ and NH₄⁺, and thus calls for a reassessment of the overall permeation mechanism in ammonium transporters.

Received for publication 8 January 2007 and in final form 26 February 2007.

Address reprint requests and inquiries to Guillaume Lamoureux, E-mail: lamourgu@cmm.upenn.edu; or Simon Bernèche, E-mail: simon.berneche@unibas.ch.

The crystal structures of *Escherichia coli* ammonium transporter AmtB (1,2) and of homologous Amt-1 (3) are providing direct insight on how proteins of the Amt/MEP/Rh family catalyze the diffusion of ammonium (NH₄⁺ and/or NH₃) through the cellular membrane. In all structures, the protein forms a narrow pore lined with hydrophobic residues including two functionally important (4) hydrogen-bonded histidine residues (H168 and H318 in AmtB), and constricted on the periplasmic side by two phenylalanine residues (F107 and F215 in AmtB, see Fig. 1). According to the current understanding, this pore is thought to allow the diffusion of ammonia (NH₃) but to prevent the permeation of water (1) and charged species such as NH₄⁺, K⁺, and Na⁺ (2). All three published x-ray diffraction studies (1–3) have found significant electronic density at the level of the two histidines, which was alternatively assigned to ammonia (1), to either ammonia or water (2), and to xenon (3). From the x-ray data alone, it is impossible to distinguish ammonia from water because both molecules have the same number of electrons. Electronic density in the hydrophobic pore has been observed in presence and absence of ammonium salt, and contradictory results were reported for similar crystallization conditions (1,2). Thus, based on available experimental data, one cannot draw a definite conclusion on the molecular species occupying the pore.

Khademi et al. (1) have proposed that AmtB binds NH₄⁺, which gets deprotonated in the periplasmic vestibule and then diffuses as NH₃ through three binding sites (adjacent to H168 and H318) according to a single-file diffusion mechanism reminiscent of permeation in potassium channels. It was thus concluded that AmtB, initially thought to be an ammonium (NH₄⁺) transporter like other similar bacterial proteins (5), was in fact an ammonia (NH₃) channel. The proposed permeation mechanism relies on the assumption

that water molecules are excluded from the hydrophobic pore, against some x-ray crystallographic data suggesting the contrary (2) (see below). To assess the validity of that mechanism, it is important to address the exact nature of the chemical species allowed in the so-called hydrophobic pore. In this letter, we report free energy molecular dynamics (MD) simulations of the AmtB transporter, using the open conformation solved by Zheng et al. (2) (PDB code 1XQE). The simulations suggest that the pore is accessible to cytoplasmic water molecules and leads to the formation of a stable water chain.

An explicit all-atom molecular system containing the AmtB monomer embedded in a DMPC bilayer was constructed following a protocol reported previously (6). Because the crystal structure does not resolve the protonation states of H168 and H318 (which are forming a strong hydrogen bond through their δ -nitrogen atoms), two different states are built: H168 donor, with the proton on N δ for H168 and on N ϵ for H318; and H168 acceptor, with the proton on N ϵ for H168 and on N δ for H318. (See Supplementary Material for details about the system and simulation protocol.)

In a first stage, both protonation states of the H168/H318 dyad are simulated for 10 ns, starting with an empty pore at the level of the two histidines. In the H168-donor system, after \sim 100 ps of simulation a first water molecule enters the pore from the cytoplasmic side, and <2 ns later a water chain fills the pore. In contrast, the H168-acceptor system never fills with water. One or two molecules may briefly reach residue H168 at the top of the pore, but a water chain is never formed. The density profiles of water molecules in the pore, accumulated for the last 8 ns of the 10-ns free simulations, are presented in Fig. 2. In the H168-acceptor case (*dashed*

line), water W1 is on average much higher in the pore and is not properly oriented to form a strong hydrogen bond with W2, which in consequence is not stabilized.

The simulations clearly indicate that the open AmtB structure 1XQE is fully accessible to water on the cytoplasmic side. This observation is contrasting with the results of previous MD studies based on the 1U7G structure (1,7). In the 1XQE structure the side chain of V314 points away from the pore (Fig. 1), while in 1U7G (and also in structure 1XQF of (2)) it partially blocks the diffusion pathway. It raises the issue of whether this conformational change plays a physiological role, or if only one of the two conformations represents a functional protein. The protonation state of the histidine dyad has also a clear impact on the stability of water molecules in the pore. While little density is observed in the case of the H168-acceptor state, the H168-donor simulation displays three pronounced density maxima at positions in striking concordance with the electron density maxima seen in the pore of x-ray structure 1XQF of Zheng et al. (2). In this x-ray study, the closed structure 1XQF is the only one for which electron density peaks could reliably be located inside the pore (F. K. Winkler, personal communication, 2006); 1XQF was obtained from crystals grown in absence of ammonium sulfate, reinforcing the idea that the observed density corresponds to water molecules. The absence of experimental electronic density peaks in the pore of 1XQE must not mean that water molecules are excluded from the pore. Rather, it may be the result of greater motional freedom of the water molecules due to the different pore structure and/or the different crystal packing resulting in different constraints on molecular motion. This could smear out the observed water electron density to noise level. Overall, the agreement

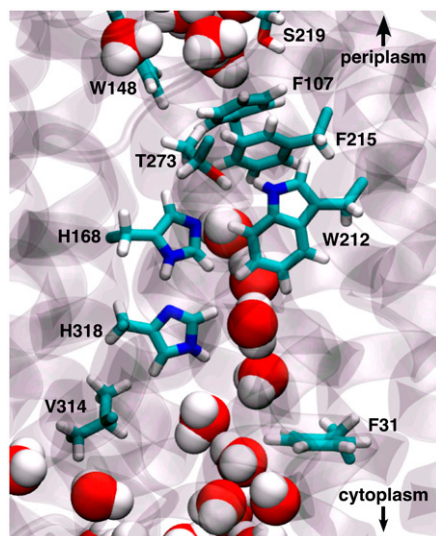


FIGURE 1 Detail of the open AmtB structure of Zheng et al. (2) (PDB code 1XQE), equilibrated with molecular dynamics. The conformation of residue V314 allows water to enter the pore and form a stable chain.

between the experimental and simulated densities suggests that the x-ray structures of Zheng et al. (2) are consistent with the presence of water molecules in the hydrophobic pore, and a H168-donor protonation state of the histidine dyad.

To confirm the somewhat anecdotal evidence obtained from the free simulations, we calculate for both protonation states the potential of mean force (PMF) of the progression of the water-front inside the pore. The PMFs are calculated using the adaptive biasing force method (8,9) implemented in the NAMD package (10). The reaction coordinate ζ used for the biasing force is the z-coordinate of the highest water molecule (the one closest to F215) relative to the center of mass of the N_ϵ atoms of H168 and H318. This reaction coordinate is therefore defined in terms of the leading water molecule, whichever it is, and the biasing force is applied on that water molecule (see Supplementary Material). For the H168-donor structure, a biased simulation of 6 ns is produced, during which the range of ζ that describes the transition from an empty pore to a water-filled pore is uniformly and repeatedly sampled. The resulting PMF is presented in Fig. 3. It displays a barrier of ~ 2 kcal/mol at the level of the CH group of H318 (between sites W2 and W3) and an absolute minimum at the level of site W1, which indicates that a fully hydrated pore is the most stable conformation. The water molecule in site W1 is in a favorable binding pocket formed by different polar and aromatic amino acids (see Fig. 1 and (2)). The PMF of Fig. 3 is different from that of a single molecule entering the pore because it includes the stabilizing effects of additional water molecules that follow the first molecule most of the time. For the H168-acceptor structure, however, the PMF obtained from 9 ns of biased simulation (see *dashed line* of Fig. 3) displays shallow minima around $\zeta \sim -3$ Å and $\zeta \sim 4.5$ Å. These positions are consistent with the water profile reported in Fig. 2 (*dashed line*), but are incommensurate with the electronic density observed for structure 1XQF. However, as the protonation state of the two histidine residues might change during the permeation process, both PMFs provide valuable information.

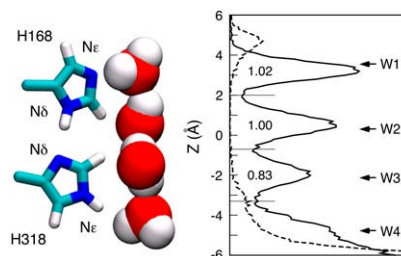


FIGURE 2 Water density profiles in the pore of AmtB, for the open structure 1XQE in the H168-donor (*solid line*) and H168-acceptor (*dashed line*) protonation states. Data is accumulated from the last 8 ns of 10-ns simulations. The average occupancy number of each peak is indicated under the curve. Arrows are showing the positions of density peaks from x-ray diffraction data of the closed structure 1XQF (2).

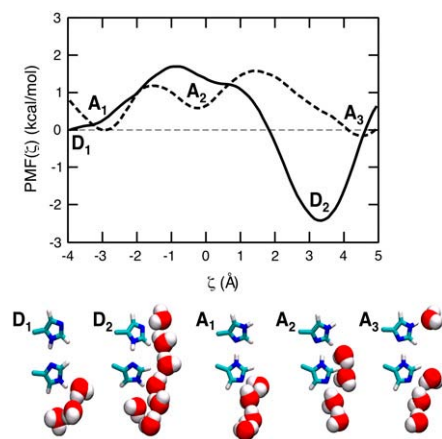


FIGURE 3 Potential of mean force of cytoplasmic water going into the empty AmtB pore of the 1XQE open structure for both protonation states. The reaction coordinate, ξ , is the z-coordinate offset of the highest permeating water molecule with respect to the center of mass of the N_ϵ atoms of H168 and H318. Molecular representations of each stable and metastable configuration are shown (H168 donor, solid line, D_1 , D_2 ; H168 acceptor, dashed line, A_1 , A_2 , A_3).

Our results support the notion that, at low ammonium concentration, the pore of the open AmtB structure is stabilizing a chain of water molecules distributed according to the profile of Fig. 2. It raises some doubts on the conduction mechanisms proposed so far (1,7,11,12); see also (13). While there is a large consensus on the fact that AmtB mainly binds NH_4^+ , which at some point gets deprotonated and diffuses as NH_3 in the hydrophobic pore, many questions remain. In the light of the results presented here, the proposed single file diffusion mechanism is far from conclusive. It also revives the semantic debate on the designation of AmtB as a transporter or a channel. If the permeation mechanism consists in the sequential binding, deprotonation, and release of one substrate molecule at a time, the term transporter might suit AmtB better. Furthermore, recent simulations of Luzhkov et al. (12) have shown that NH_4^+ is not stable in a pore filled with NH_3 . However, because cations are better solvated in water than in ammonia, the AmtB water-filled pore is calling for a reexamination of NH_4^+ affinity of site W1 (equivalent to site AM2 in the structure of (1)), which might bring new insights on the ammonium deprotonation site, and in fine on the permeation mechanism.

Finally, given that electrophysiological measurements are suggesting that some AmtB homologs, notably in plants, are capable of co-transporting protons (14), the idea that the pore of ammonium transporter might stabilize water molecules is appealing. Indeed, it is well known that, in confined space, water molecules can form highly ordered chains and transport protons using the Grotthuss mechanism (15). A similar proton shuttling mechanism can take place in an ammonia chain, but it may not be as efficient in the context of a narrow hydrophobic pore (16).

SUPPLEMENTARY MATERIAL

An online supplement to this letter can be found by visiting BJ Online at <http://www.biophysj.org>.

ACKNOWLEDGMENTS

We thank Fritz K. Winkler, Xiao-Dan Li, Arnaud Javelle, and Jérôme Hénin for helpful discussions.

G. L. is a fellow of the Fonds Québécois de la Recherche sur la Nature et les Technologies. S. B. is a fellow of the International Human Frontier Science Program Organization. Computational resources were provided by the National Center for Supercomputing Applications and the Basel Computational Biology Centre. This work was funded in part by National Institutes of Health grant No. GM 40712.

REFERENCES and FOOTNOTES

1. Khademi, S., J. O'Connell III, J. Remis, Y. Robles-Colmenares, L. J. W. Miercke, and R. M. Stroud. 2004. Mechanism of ammonia transport by Amt/MEP/Rh: structure of AmtB at 1.35 Å. *Science*. 305:1587–1594.
2. Zheng, L., D. Kostrewa, S. Bernèche, F. K. Winkler, and X.-D. Li. 2004. The mechanism of ammonia transport based on the crystal structure of AmtB of *Escherichia coli*. *Proc. Natl. Acad. Sci. USA*. 101:17090–17095.
3. Andrade, S. L. A., A. Dickmanns, R. Ficner, and O. Einsle. 2005. Crystal structure of the archaeal ammonium transporter Amt-1 from *Archaeoglobus fulgidus*. *Proc. Natl. Acad. Sci. USA*. 102:14994–14999.
4. Javelle, A., D. Lupo, L. Zheng, X.-D. Li, F. K. Winkler, and M. Merrick. 2006. An unusual twin-His arrangement in the pore of ammonia channels is essential for substrate conductance. *J. Biol. Chem.* 281:39492–39498.
5. Kleiner, D. 1985. Bacterial ammonium transport. *FEMS Microbiol. Rev.* 32:87–100.
6. Bernèche, S., M. Nina, and B. Roux. 1998. Molecular dynamics simulation of melittin in a dimyristoylphosphatidylcholine bilayer membrane. *Biophys. J.* 75:1603–1618.
7. Bostick, D. L., and C. L. Brooks. 2007. Deprotonation by dehydration—the origin of ammonium sensing in the AmtB channel. *PLoS Comp. Biol.* doi: 10.1371/journal.pcbi.0030022.
8. Darve, E., and A. Pohorille. 2001. Calculating free energies using average force. *J. Chem. Phys.* 115:9169–9183.
9. Hénin, J., and C. Chipot. 2004. Overcoming free energy barriers using unconstrained molecular dynamics simulations. *J. Chem. Phys.* 121: 2904–2914.
10. Phillips, J. C., R. Braun, W. Wang, J. Gumbart, E. Tajkhorshid, E. Villa, C. Chipot, R. D. Skeel, L. Kale, and K. Schulten. 2005. Scalable molecular dynamics with NAMD. *J. Comput. Chem.* 26:1781–1802.
11. Lin, Y., Z. Cao, and Y. Mo. 2006. Molecular dynamics simulations on the *Escherichia coli* ammonia channel protein AmtB: mechanism of ammonia/ammonium transport. *J. Am. Chem. Soc.* 128:10876–10884.
12. Luzhkov, V. B., M. Almlöf, M. Nervall, and J. Åqvist. 2006. Computational study of the binding affinity and selectivity of the bacterial ammonium transporter AmtB. *Biochemistry*. 45:10807–10814.
13. Nygaard, T. P., C. Rovira, G. H. Peters, and M. Ø. Jensen. 2006. Ammonium recruitment and ammonia transport by *E. coli* ammonia channel AmtB. *Biophys. J.* 91:4401–4412.
14. Mayer, M., G. Schaaf, I. Mouro, C. Lopez, Y. Colin, P. Neumann, J.-P. Cartron, and U. Ludewig. 2006. Different transport mechanisms in plant and human AMT/Rh-type ammonium transporters. *J. Gen. Physiol.* 127:133–144.
15. Decoursey, T. E. 2003. Voltage-gated proton channels and other proton transfer pathways. *Physiol. Rev.* 83:475–579.
16. Zoete, V., and M. Meuwly. 2004. On the influence of semirigid environments on proton transfer along molecular chains. *J. Chem. Phys.* 120:7085–7094.